JACS
JOURNAL OF THE AMERICAN CHEMICAL SOCIETY
Communication
pubs.acs.org/JACS

Development of Metal–Organic Nanotubes Exhibiting Low-Temperature, Reversible Exchange of Confined "Ice Channels"

Daniel K. Unruh, Kyle Gojdas, Anna Libo, and Tori Z. Forbes*

Department of Chemistry, University of Iowa, Chemistry Building W374, Iowa City, Iowa 52242, United States

Supporting Information

ABSTRACT: Nanotubular materials have unique water transport and storage properties that have the potential to advance separations, catalysis, drug delivery, and environmental remediation technologies. The development of novel hybrid materials, such as metal–organic nanotubes (MONs), is of particular interest, as these materials are amenable to structural engineering strategies and may exhibit tunable properties based upon the presence of inorganic components. A novel metal–organic nanotube, $(C_4H_{12}N_2)_{0.5}[(UO_2)(H\mathit{ida})(H_2\mathit{ida})]\cdot 2H_2O$ (**UMON**) (*ida* = iminodiacetate), that demonstrates the possibilities of these types of hybrid compounds has been synthesized via a supramolecular approach. Single-crystal X-ray diffraction of the compound revealed stacked macrocyclic arrays that contain highly ordered water molecules with structural similarities to the "ice channels" observed in single-walled carbon nanotubes. Nanoconfinement of the water molecules may be the cause of the unusual exchange properties observed for **UMON**, including selectivity to water and reversible exchange at low temperature (37 °C). Similar properties have not been reported for other inorganic or hybrid compounds and indicate the potential of MONs as advanced materials.

The ability to store or convey solutions with nanoscale precision is fundamental to the control and selectivity of biological systems[1,2] and the development of novel nanomaterials for advanced separations technologies; however, the current understanding of nanoconfined water, particularly its structural configuration, is limited. Hybrid compounds hold significant promise in the development of novel materials with controllable water transport properties, as they have tunable hydrophobic and hydrophilic components.[3−5] Metal–organic nanotubes (MONs) are a relatively rare class of hybrid compounds that show potential for unique exchange properties, but synthetic challenges currently limit their development.[3,6−9] Using a supramolecular approach, we recently synthesized a novel MON, $(C_4H_{12}N_2)_{0.5}[(UO_2)(H\mathit{ida})(H_2\mathit{ida})]\cdot 2H_2O$ (**UMON**) (*ida* = iminodiacetate), that exhibits a unique structural arrangement of the water molecules within the interior of the nanotube. This novel material possesses unusual properties, including rapid, reversible exchange of the nanoconfined water molecules under near-ambient conditions (37 °C) and specific selectivity to water uptake within the nanotubes.

UMON was synthesized under ambient conditions by dissolving uranyl nitrate, piperazine, and iminodiacetic acid in a 1:1 water/methanol solution. In less than 3 days, large single crystals were formed in over 95% yield based upon U, and subsequent structural characterization of the compound was performed at −173.15 °C on a Nonius Kappa CCD single-crystal X-ray diffractometer equipped with an Oxford low-temperature cryostat. The material crystallizes in the trigonal space group $P\bar{3}$ with a = 22.3054(13) Å, c = 6.6297(5) Å, and V = 2956.6(3) Å^3.

The compound contains one crystallographically unique U(VI) metal center bonded to two oxygen atoms, creating the nearly linear uranyl cation $(UO_2)^{2+}$ that is further chelated in a tridentate fashion through the equatorial plane by an *ida* ligand. Pentagonal bipyramidal coordination about the uranyl cation results from further complexation by additional *ida* linker molecules, connecting neighboring U(VI) polyhedra into a cyclic hexameric macrocycle (Figure 1a). The significant corrugation observed within the macrocycle may be promoted by hydrogen bonding between the doubly protonated N atoms on the *ida* linkers and the carboxylate functional groups on the neighboring rings, leading to the formation of the nanotubular array (Figure 1b). The overall charge on each individual macrocycle is 6−, and the electrical neutrality of the compound is maintained by the presence of piperazinium cations located between the nanotubular structures.

The internal diameter of the nanotubular array was measured as 1.2 nm on the basis of the distance between opposing uranyl O atoms, and the material has a calculated pore space of 2447 Å^3 per unit cell. Water molecules are located within the interiors of the nanotubes at two crystallographically unique positions (OW1 and OW2) and form hexagonal rings with chair configurations based upon the symmetry-equivalent positions. The OW1 site is well-resolved, with an interatomic distance of 2.792 Å between adjacent water molecules (Figure 1c). A second hexagonal array of water molecules (OW2) is located 2.850 Å from the first ring and possesses a slightly larger diameter, with neighboring O atoms separated by 3.200 Å. Modeling of the OW2 atoms as thermal ellipsoids indicated fairly significant anisotropy and disorder at that atomic position, which was supported by further analysis of the two-dimensional (2D) electron density maps of the interior of the nanotubes [see the Supporting Information (SI)].

Hydrogen atoms for the OW1 site were located following refinement of the overall structure with H–O–H bond angles

Received: January 10, 2013
Published: May 3, 2013

dx.doi.org/10.1021/ja400303f | J. Am. Chem. Soc. 2013, 135, 7398−7401

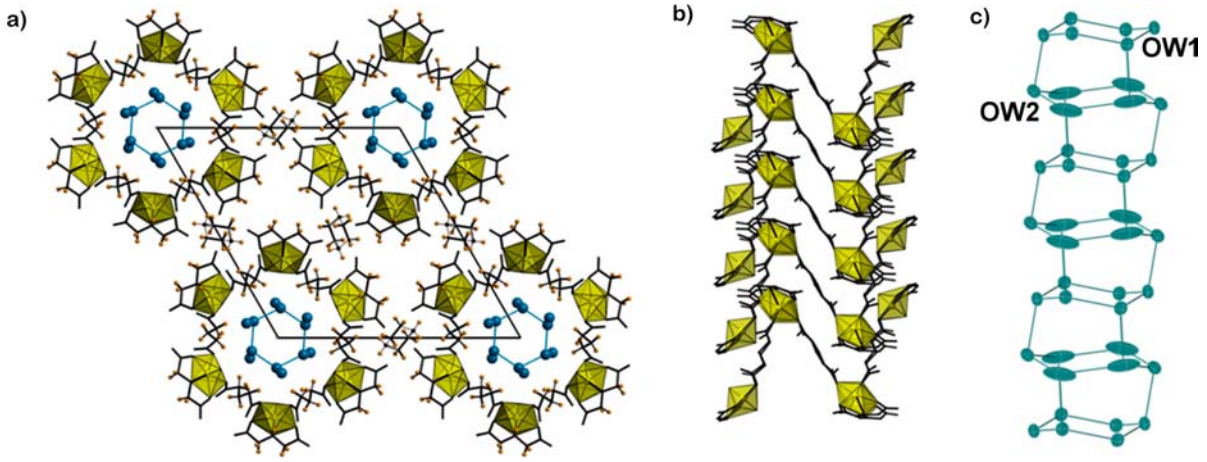

Figure 1. UMON contains hexagonally packed water molecules within nanotubular structures. (a) Each nanotube is composed of uranyl pentagonal bipyramids (yellow-green polyhedra) that are linked through iminodiacetate (*ida*) ligands (black stick models with H atoms displayed as orange spheres). The structure is charge-balanced by piperazinium cations, and water molecules (teal spheres) are located in the interiors of the nanotubes. (b) Linkages between the metal centers create corrugated macrocycles that stack into nanotubular arrays through supramolecular interactions. (c) Two crystallographically unique water molecules are located within the nanotubular structure, forming a structural network with similarities to ice Ih.

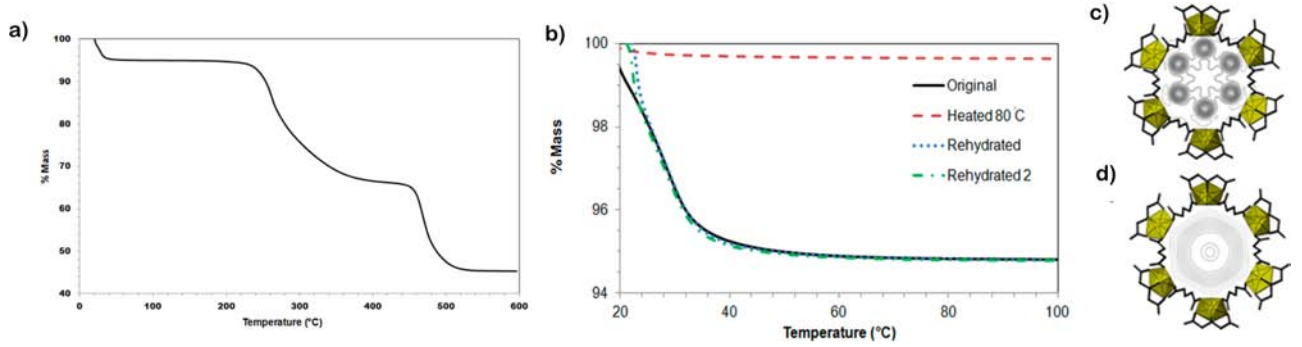

Figure 2. Unique water exchange properties are present in the **UMON** material, as observed by TGA and single-crystal XRD. (a) The water molecules within the interior of the nanotube were completely removed from the material at 37 °C, but the crystallinity was maintained until 250 °C. (b) Removal of the water from a sample that had previously been heated to 80 °C was confirmed by the absence of a significant mass loss from the material up to 100 °C. **UMON** material could be rehydrated multiple times by equilibrating the sample on the benchtop for 30 min, as evidenced by mass loss below 50 °C. (c) The presence of water in the original sample was demonstrated by the 2D electron density map of the OW1 site, which illustrates the hexagonal array of water in the interior of the nanotube. (d) Single-crystal XRD data were collected from a **UMON** crystal heated to 80 °C, and no significant electron density was found within the nanotubes, confirming the results of the mass loss experiment.

within the water molecule of 113.2° and H···O distances of 1.815 and 1.867 Å to neighboring OW1 and OW2 groups, respectively. The significant disorder of the OW2 site prevented accurate placement of the H atoms on the water molecules, and thus, the complete hydrogen-bonding network of the water molecules could not be determined. However, the position of the O atoms and the partial hydrogen-bonding network observed in the structural analysis of **UMON** are similar to those observed in the most common polymorph of ice, hexagonal ice I (ice Ih), which consists of sheets of tessellating hexamers in chair conformations linked together through an extensive hydrogen-bonding network. The average O−H···O distance of 2.75 Å and H−O−H bond angle of 109° for ice Ih are similar to those observed within **UMON**.

While the presence of water molecules in hybrid materials is quite common, the solvent is generally disordered or strongly bonded to a metal center.[3,7] **UMON** differs from previously synthesized hybrid MONs and metal−organic frameworks (MOFs) because of the limited interaction between the U(VI) polyhedra and the confined water molecules. The oxygen atoms of the uranyl moiety point toward the interior of the nanotube but are strongly bonded to the metal center, limiting their participation in hydrogen bonding. Additional interactions between the aliphatic backbone of the *ida* linker and the water molecules may occur, but they provide a more hydrophobic character that is reminiscent of the presence of water molecules in single-walled carbon nanotubes (SWCNTs).

Similar ice channels or "ice nanotubes", have been observed in hydrated SWCNTs with internal diameters of 0.8−1.5 nm at temperatures below −50 °C.[10,11] Because of the fibrous nature of the material, the arrangement of the water molecules within SWCNTs could not be determined experimentally, but it has been the subject of numerous computational studies.[12] Classical molecular dynamics (MD) simulations indicated that the ice nanotubes can form a variety of configurations depending on the overall diameter of the tube, the temperature and pressure regimes, and the choice of modeling parameters. The most frequently predicted structural features are rings that contain four, six, or eight water molecules,[13,14] although helical and cubic configurations have also been proposed.[15−17] Under ambient conditions (25 °C, 1 bar), the ice Ih structure was predicted to exist in SWCNTs with a van der Waals diameter of

dx.doi.org/10.1021/ja400303f | J. Am. Chem. Soc. 2013, 135, 7398−7401

8.6 Å but was notably absent from larger tubes.[12,13] Additional computational studies suggested that structural ordering in larger SWCNTs (1−2 nm) occurs only when the temperature is decreased below −60 °C, at which point the water molecules within the interior of the nanotubes form octagonal arrays.[14]

Unlike those in SWCNTs, the ice channels within **UMON** could be observed by single-crystal X-ray diffraction (XRD) at −173 °C but persisted when the data were collected at −60 and 25 °C (Figure S3 in the SI). Each of the individual OW1 molecules within the hexagonal ring could be distinguished for each data set, but the electron density was more diffuse and the disorder of the OW2 site became more pronounced with increasing temperature; thus, the structural ordering of the ice channels within **UMON** can be somewhat maintained beyond the normal melting point of bulk ice. The phase transition between liquid water and solid ice in SWCNTs has been observed at −50 °C and displays a continuous structural transformation, suggesting the presence of a quasi-liquid state over a sizable temperature range.[10,11,18]

UMON possesses unique water exchange properties, as first discovered by thermogravimetric analysis (TGA) of the compound (Figure 2a). The initial mass loss at 37 °C in the TGA data corresponds to the complete removal of the water molecules, whereas the second and third weight losses at 250 and 450 °C are due to the combustion of the organic constituents, indicating relatively good thermal stability of the compound. Removal of the water molecules from **UMON** at such a low temperature is quite surprising given that other MONs and related inorganic materials typically release structural water between 80 and 200 °C.[7,9,19,20] The average mass loss associated with the water molecules based upon six separately prepared **UMON** samples was 5.54 ± 0.30%, indicating that the overall formula is $(C_4H_{12}N_2)_{0.5}[(UO_2)(H\mathit{ida})(H_2\mathit{ida})]\cdot 1.9H_2O$, confirming the formula obtained by single-crystal XRD. After release of the water, the crystallinity was maintained, as demonstrated by single-crystal analysis of the heated sample (R_1 = 2.16%, see the SI for more details).

The diffraction experiment on the heated material indicated no significant electron density within the interior of the nanotubes (Figure 2d), suggesting complete removal of the water from the interior of the nanotubes. The absence of water within the heated nanotubes was corroborated by TGA, as no mass loss was observed from 25 to 200 °C (Figure 2b). Rehydration of **UMON** was spontaneous when the sample was cooled to room temperature, and the presence of the ordered water in the nanotube after the heat cycle was again confirmed by single-crystal XRD and TGA analysis. The water desorption/adsorption cycle could be repeated multiple times with no apparent loss of crystallinity or overall stability of the material.

UMON is also selective to water, showing little exchange with other polar and nonpolar solvents. Hydrated **UMON** crystals were placed into the polar solvent dimethyl sulfoxide (DMSO) for several hours, and single-crystal XRD studies of the exchanged material showed no significant electron density within the interior of the nanotubes (Figure 3a,b), which suggested complete removal of water and little uptake of the nonaqueous solvent. The removal of water from **UMON** crystals immersed in DMSO was also corroborated by a gradual 1% mass loss when the sample was heated to 200 °C, instead of the abrupt mass loss below 50 °C observed during heating of the hydrated material. The percent mass loss data indicated that 0.08 mol of DMSO/mol of U was absorbed by the sample, in

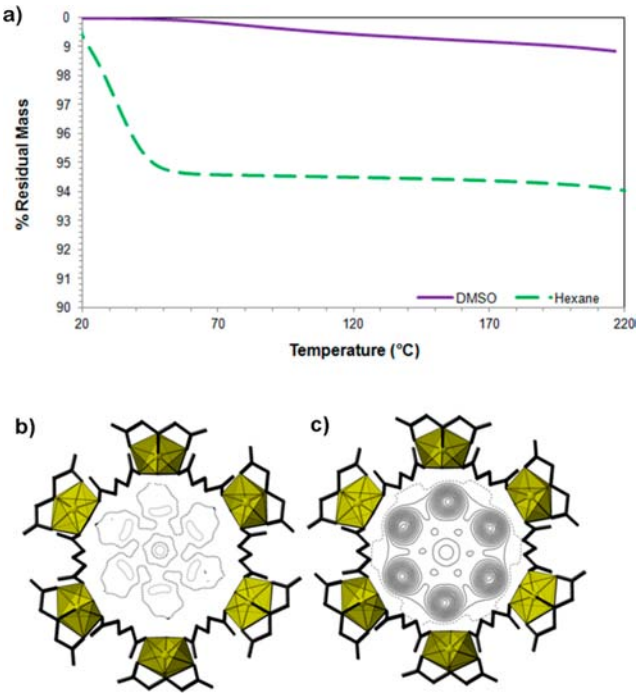

Figure 3. UMON samples placed in polar (DMSO) or nonpolar (hexane) solvent result in significant changes in the hydration of the material. (a) TGA of the **UMON** sample placed in DMSO suggested removal of the water molecules with only a small uptake of the solvent (1 wt %). However, samples placed in hexane exhibited a mass loss similar to the fully hydrated material (5.53%), suggesting no exchange of the confined water molecules with the surrounding solvent. (b) The 2D electron density map of the OW1 site in the **UMON** sample placed into DMSO displays little electron density, whereas (c) the sample placed into hexane contains six well-ordered water molecules, confirming the TGA analyses.

contrast to the 2 mol of H_2O/mol of U in the original **UMON**. Hydrated **UMON** crystals placed in hexane exhibited no exchange, as characterized by XRD and TGA (Figure 3a,c). Additional experiments on evacuated UMON samples also indicated no significant uptake of either DMSO or hexane solvent.

Solvent exchange is fairly typical for porous hybrid materials but generally results in occupation of the channels by molecules with similar hydrophilic or hydrophobic properties. Potentially, the release of the water from hydrated **UMON** with little uptake of the DMSO solvent could be caused by the presence of the ice channels, although the exact physical or chemical characteristics that govern this exchange are still in question. This phenomenon has not been experimentally observed with hydrated SWCNTs, but MD simulations of the conduction of water through 1.0 nm diameter nanotubes found that the channel occupancy and conductivity can be tuned by changing the polarity of the solvent.[21]

UMON offers the first structural glimpse into the presence of confined ice channels within nanomaterials and could lead to the development of new hybrid materials that offer exceptional control over water release and uptake for advanced applications.[21−23] The successful crystallization of **UMON** offers a novel approach to the rational design of MON materials, as it is the first hybrid compound to contain stacked macrocycle arrays as the fundamental building units for the nanotubular design. Supramolecular interactions between

dx.doi.org/10.1021/ja400303f | J. Am. Chem. Soc. 2013, 135, 7398−7401

macrocyclic components have previously been reported for the self-assembly of organic-based nanotubes, including cyclic peptides, calix[4]arenes, cyclodextrins, crown ethers, and macrooligolides, but have not been utilized for hybrid materials.[2,24−26] Hydrogen bonding of the macrocyclic arrays within **UMON** leads to a surprisingly robust material that is comparable to other hybrid MON and MOF materials. Combined with their tunable components, MON materials hold great promise for the development of new compounds with unique solvent storage and exchange properties for advanced technological applications.

■ ASSOCIATED CONTENT

Supporting Information

Description of synthesis, additional structural details, crystallographic data (CIF), difference Fourier maps, elemental analysis, powder X-ray diffraction data, and Raman and IR spectra. This material is available free of charge via the Internet at http://pubs.acs.org.

■ AUTHOR INFORMATION

Corresponding Author

tori-forbes@uiowa.edu

Notes

The authors declare no competing financial interest.

■ ACKNOWLEDGMENTS

We thank the UI NMR Facility and Dr. Fu Chen for MAS NMR data collection and analysis. In addition, we thank the UI Central Microscopy Facility for use of the Raman spectrometer, Professor Edward Gillan, and Dr. Dale Swenson. This work was supported by the Nuclear Regulatory Commission (Faculty Development Grant NRC-HQ-12-G-38-0041) and the University of Iowa College of Liberal Arts and Sciences.

■ REFERENCES

(1) Tajkhorshid, E.; Nollert, P.; Jensen, M. Ø.; Miercke, L. J. W.; O'Connell, J.; Stroud, R. M.; Schulten, K. *Science* **2002**, *296*, 525.
(2) Hu, C. B.; Chen, Z. X.; Tang, G. F.; Hou, J. L.; Li, Z. T. *J. Am. Chem. Soc.* **2012**, *134*, 8384.
(3) Thanasekaran, P.; Suo, T.-T.; Lee, C.-H.; Lu, K.-L. *J. Mater. Chem.* **2011**, *21*, 13140.
(4) Wang, W.; Dong, X.; Nan, J.; Jin, W.; Hu, Z.; Chen, Y.; Jiang, J. *Chem. Commun.* **2012**, *48*, 7022.
(5) Dutta, A.; Patra, A. K.; Bhaumik, A. *Microporous Mesoporous Mater.* **2012**, *155*, 208.
(6) Panda, T.; Kundu, T.; Banerjee, R. *Chem. Commun.* **2012**, *48*, 5464.
(7) (a) Reinsch, H.; Marszałek, B.; Wack, J.; Senker, J.; Gil, B.; Stock, N. *Chem. Commun.* **2012**, *48*, 9486. (b) Kumar, S.; Doctorovich, F. *Inorg. Chem. Commun.* **2012**, *15*, 33. (c) Bernin, M.; Brusau, E.; Narda, G.; Echeverria, G.; Fantoni, A.; Punte, G.; Ayala, A. *Polyhedron* **2012**, *31*, 729. (d) Dey, R.; Haldar, R.; Maji, T.; Ghoshal, D. *Cryst. Growth Des.* **2011**, *11*, 3905.
(8) Otsubo, K.; Wakabayashi, Y.; Ohara, J.; Yamamoto, S.; Matsuzaki, H.; Okamoto, H.; Nitta, K.; Uruga, T.; Kitagawa, H. *Nat. Mater.* **2011**, *10*, 291.
(9) Zhao, B.; Cheng, P.; Chen, X.; Cheng, C.; Shi, W.; Liao, D.; Yan, S.; Jiang, Z. *J. Am. Chem. Soc.* **2004**, *126*, 3012.
(10) Maniwa, Y.; Kataura, H.; Abe, M.; Udaka, A.; Suzuki, S.; Achiba, Y.; Kira, H.; Matsuda, K.; Kadowaki, H.; Okabe, Y. *Chem. Phys. Lett.* **2005**, *401*, 534.
(11) Koga, K.; Gao, G. T.; Tanaka, H.; Zeng, X. C. *Nature* **2001**, *412*, 802.
(12) Alexiadis, A.; Kassinos, S. *Chem. Rev.* **2008**, *108*, 5014.
(13) Mashl, R. J.; Joseph, S.; Aluru, N. R.; Jakobsson, E. *Nano Lett.* **2003**, *3*, 589.
(14) Kolesnikov, A. I.; Loong, C.-K.; de Souza, N. R.; Burnham, C. J.; Moravsky, A. P. *Physica B: Condens. Matter* **2006**, *385−386*, 272.
(15) Striolo, A.; Chialvo, A. A.; Gubbins, K. E.; Cummings, P. T. *J. Chem. Phys.* **2005**, *122*, No. 234712.
(16) Liu, Y. C.; Wang, Q.; Wu, T.; Zhang, L. *J. Chem. Phys.* **2005**, *123*, No. 234701.
(17) Liu, Y. C.; Wang, Q.; Zhang, L.; Wu, T. *Langmuir* **2005**, *21*, 12025.
(18) Maniwa, Y.; Kataura, H. *Top. Appl. Phys.* **2010**, *117*, 247.
(19) Floquet, N.; Coulomb, J. P.; Dufau, N.; Andre, G. *J. Phys. Chem. B* **2004**, *108*, 13107.
(20) Chai, X.-C.; Sun, Y.-Q.; Lei, R.; Chen, Y.-P.; Zhang, S.; Cao, Y.-N.; Zhang, H.-H. *Cryst. Growth Des.* **2010**, *10*, 658.
(21) Hummer, G.; Rasaiah, J. C.; Noworyta, J. P. *Nature* **2001**, *414*, 188.
(22) Kohmoto, S.; Okuyama, S.; Yokoto, N.; Takahashi, M.; Kishikawa, K.; Masu, H.; Azumaya, I. *Cryst. Growth Des.* **2011**, *11*, 3698.
(23) Fei, Z.; Geldbach, T. J.; Zhao, D.; Scopelliti, R.; Dyson, P. J. *Inorg. Chem.* **2005**, *44*, 5200.
(24) Carrillo, R.; Lopez-Rodriguez, M.; Martin, V. S.; Martin, T. *CrystEngComm* **2010**, *12*, 3676.
(25) Ghadiri, M. R.; Granja, J. R.; Milligan, R. A.; McRee, D. E.; Khazanovich, N. *Nature* **1993**, *366*, 324.
(26) Hui, J. K. H.; Frischmann, P. D.; Tso, C.-H.; Michal, C. A.; MacLachlan, M. J. *Chem.—Eur. J.* **2010**, *16*, 2453.